Contents lists available at Science-Gate

International Journal of Advanced and Applied Sciences

Journal homepage: http://www.science-gate.com/IJAAS.html

Equation of state of Krypton gas in the temperature-range 120-130 K

Amal F. Al-Maaitah *, Amer D. Al-Oqali

Department of Physics, Mutah University, Mutah, Jordan

ARTICLE INFO

Article history:
Received 26 January 2022
Received in revised form
29 April 2022
Accepted 24 May 2022

Keywords:
Krypton gas
Quantum second virial coefficient
Internal energy
Enthalpy
Compressibility

ABSTRACT

This study aims to find out an equation of state for Krypton gas (Kr) in the temperature range 120–130 K and to calculate some of its thermodynamic properties. The virial equation of state for Krypton gas (Kr) is constructed using the quantum second virial coefficient (B_q). The Beth–Uhlenbeck formula is used to calculate the quantum second virial coefficient B_q in the temperature range 120–130 K at different number densities. The pressure-volume-temperature behavior of Kr gas is carefully investigated, from which the phase (gas-liquid) transition is predicted. Some of the thermodynamic properties; the internal energy, enthalpy, and Helmholtz free energy are calculated for a number density of 4×1025 atoms/m^3 using the quantum second virial coefficient. Our results show that the deviation from ideality becomes most significant at low temperatures and increases with increasing number density. Our results for the quantum second virial coefficient are in good agreement with previous results.

1. Introduction

Krypton (Kr) is a noble gas with the atomic number of 36 and has an electronic structure of a fully occupied d-shell. Its melting point is 115.78 K and has a boiling point of 119.735 K. There are no radioactive isotopes of krypton found in nature. Kr is one of the rarest gases in the Earth's atmosphere. It is extracted by distillation of air that has been cooled until it is a liquid. Because krypton is so rare (and thus expensive), it has limited use. The gas is injected into some incandescent light bulbs because it extends the life of the tungsten filament that makes those bulbs glow. It is also used in some flash lamps used for high-speed photography. Hence, the study of the thermodynamic properties of krypton gas is of scientific significance.

The main goals of this study are to find out an equation of state for Kr gas and to calculate some of its thermodynamic properties in the temperature range 120–130 K at various densities using the Galitskii-Migdal Feynman (GMF) formalism (Ghassib et al., 1976; Bishop et al., 1976; Joudeh et al., 2010; Ghassib et al., 2014; Mosameh et al., 2014). This formalism can be viewed as an independent-pair model dressed by a many-body medium. The main outcome of GMF formalism for the present purposes is the phase shifts for the input interatomic potential. It should be noted that our phase shifts depend on the temperature and density of the medium. These, in turn, are inserted into the Beth-Uhlenbeck formula to determine the quantum second virial coefficient Bq. The equation of state describing the pressure-volume-temperature (P-V-T) behavior of the system and other thermodynamic properties is then followed according to standard recipes. The equation of state of gases at low densities is an important source of information on intermolecular forces since the coefficients of the virial form of the equation of state are the physical properties that are linked most directly to the potential of these forces (Weir et al., 1967).

The quantum second virial coefficient is of great interest in many industrial applications (Oh, 2010; Garberoglio et al., 2012). It is widely used in the determination of thermodynamic quantities (Al-Maaitah et al., 2016; Akour et al., 2018; Al-Obeidat, 2021). It determines the degree of 'nonideality' of the gaseous system. This coefficient is used to give a good approximation to the equation of the state of real gases. Also, it can act as a predictor of the possible formation of small clusters (Sandouqa, 2018; Al-Maaitah et al., 2019). In some cases, it can even be invoked to predict the critical temperature (Vliegenthart and Lekkerkerker, 2000; Nezbeda and Smith, 2004).

* Corresponding Author.
Email Address: amal.almaaitah@yahoo.com; amal_almaaita@mutah.edu.jo (A. F. Al-Maaitah)
https://doi.org/10.21833/ijaas.2022.08.018
Corresponding author's ORCID profile:
https://orcid.org/0000-0002-6561-1676

As for previous studies in this field: An ab initio potential was used in computer simulations to study the thermophysical properties of krypton gas over a wide range of densities and temperatures (Dardi and Dahler, 1992). An apparatus of the Burnett type was built to measure accurately the second virial coefficients for gases at low temperatures (Weir et al., 1967). For Kr, the second virial coefficient B was measured in the T range 110–225 K, with absolute accuracies from 0.001 to 0.01 m^3 $kmol^{-1}$. The rapid fall of B at low T implied a deep well in the binary potential. Also, B, as well as the transport properties, for the dilute gas formed of monatomic Kr was calculated at low temperatures when the quantum effects are very important and for moderate and high temperatures using the Chapman-Enskog model (Benseddik et al., 2014). Furthermore, Al-Maaitah (2018) calculated the quantum second virial coefficient for krypton gas using ab initio potential, Barker et al. potential, and Morse potential. Agreement with experiments was good though not perfect. Bq for Kr was determined in the temperature-range 0.01–10 K in the zero-density limit using the HFD-B potential (Sandouqa et al., 2020). The general behavior of Bq is the same as that of the HFD-B potential itself; there seems to be an almost one-to-one correspondence between the respective repulsive, attractive, and 'minimum' regions.

The paper is organized as follows. The theoretical framework is outlined in Section 2. The results are presented and discussed in Section 3. They are displayed in figures and tables. The paper concludes with some closing remarks in Section 4.

2. Theoretical framework

2.1. Quantum second virial coefficient Bq

The main GMF output is the many-body phase shifts, which are then used to compute the corresponding quantum second virial coefficient B_q and other thermodynamic quantities. The GMF integral equation for the T-matrix is solved by the matrix inversion technique (Ghassib et al., 1976; Bishop et al., 1976). This technique has been greatly improved over the years. The phase shifts are related to B_q through the Beth–Uhlenbeck formula (Seguin et al., 1987). This is given by:

$$B_q(T) = B_{ideal} + B_{bound} + B_{Phase} \quad (1)$$

here, B_{ideal} is the quantum ideal-gas term, which is important in the low-temperature region, but goes to zero with increasing temperature. It is given by:

$$B_{ideal} = -\frac{\lambda^3}{2^{5/2}} = -\frac{1}{2^{5/2}}\left(\frac{2\pi\hbar^2}{mk_BT}\right)^{3/2} \quad (2)$$

where, λ is the thermal de Broglie wavelength. The bound-state contribution B_{bound} is given by:

$$B_{bound} = -2^{3/2}\lambda^3 \sum_{E_B}\left(e^{-\beta E_B} - 1\right) \quad (3)$$

This term is very small and can be neglected. The last term, B_{Phase} represents the contribution of the scattering-state. It is given by:

$$B_{phase} = -\frac{2^{3/2}\lambda^5}{\pi^2} \times \int_0^\infty dk\, k \sum_{l(even)}^{\infty}(2l+1)\delta_l^E(k)e^{-\beta E(k)}, \quad (4)$$

where, $\delta_l^E(k)$ is the effective ℓ-partial phase shift corresponding to energy $E(k) = \hbar^2k^2/2m$.

In this paper, the 'natural' system of units is used, i.e., $\hbar = k = m = 1$. The conversion factor $\hbar^2/m$ for Kr gas is 0.5781 K.Å^2.

2.2. Interatomic potential

The only input needed is the binary potential V(r) which has been chosen as the HFD-B. Its general form is given by (Aziz and Slaman,1986):

$$V(r) = \varepsilon V^*(x) \quad (5)$$

$$V^*(x) = Aexp(-\alpha x + \beta x^2) - \left\{\frac{C_6}{x^6} + \frac{C_8}{x^8} + \frac{C_{10}}{x^{10}}\right\}F(x) \quad (6)$$

$$F(x) = \begin{cases} exp - \left[\left\{\frac{D}{x} - 1\right\}^2\right], & x < D \\ 1, & x > D \end{cases} \quad (7)$$

where, $x \equiv \frac{r}{r_m}$; $r_m = 4.008$Å; $D = 1.28$; $A = 1.10146811 \times 10^5$; $= \alpha = 9.39490495$; $\beta = -2.32607647$; $C_6 = 1.08822526$; $C_8 = 0.53911567$ $C_{10} = 0.42174119$; ε=210.2K.

3. Results and discussions

3.1. Second virial coefficient

Our results for the quantum second virial coefficient in the T-range 120-130 K are summarized in Table 1 and Fig. 1 for the HFD-B potential. It is clear that B_q is negative for our whole T-range and it increases with increasing T (becoming less negative). A negative B_q means that the overall interaction is attractive.

$B_q(T)$ was a good pointer to show the effect of the interatomic potential on the thermodynamic properties, especially the pressure. For low T, the mean energies of the atoms in the gas are of the same order of magnitude as the depth of the potential well, resulting in an increase in the attractive forces between the interacting atoms; these spend most of their time in the attractive region of the potential. This results in a decrease in the gas pressure which leads to a negative $B_q(T)$. For high T, the average energies of the atoms increase and become large in comparison to the maximum energy of attraction. Therefore, the predominant contribution to $B_q(T)$ arises from the repulsive portion of the potential. This causes an increase in the gas pressure and, hence, $B_q(T)$ becomes less negative (Al-Maaitah et al., 2016). B_q nearly does not change at low the number density n but starts to decrease as n increases. Clearly, Kr gas exhibits small quantum effects in the temperature range considered.

Table 1 displays a comparison of our results with experimental ones. Clearly, the GMF results are becoming closer to experimental results.

Table 1: The quantum second virial coefficient B_q (cc/mol) as a function of the temperature T [K] at different number densities n [atoms/ m^3], for HFD-B potential. Some previous experimental results are included for comparison purposes

T[K]	$Bq(T)_{at}$ $n=4\times10^{20}$	$Bq(T)_{at}$ $n=4\times10^{22}$	$Bq(T)_{at}$ $n=4\times10^{25}$	$Bq(T)_{at}$ $n=4\times10^{27}$	$Bq(T)_{at}$ $n=4\times10^{29}$	$B(T)_{exp.}$ (Sengers et al., 1971)	$B(T)_{exp.}$ (Byrne et al., 1968)
120	-306.12	-306.90	-308.10	-311.76	-315.10	-307.80	-307.90
122	-297.66	-299.32	-302.46	-308.34	-309.84	-298.61	
124	-291.30	-292.61	-294.85	-301.69	-303.89	-288.80	-287.50
126	-285.43	-287.10	-290.70	-295.76	-296.83	-280.00	
128	-268.01	-273.62	-281.13	-290.58	-296.26	-271.60	
129	-263.13	-265.32	-274.50	-285.33	-290.77	-264.99	-265.40
130	-259.21	-263.87	-265.24	-279.89	-286.91	-263.70	

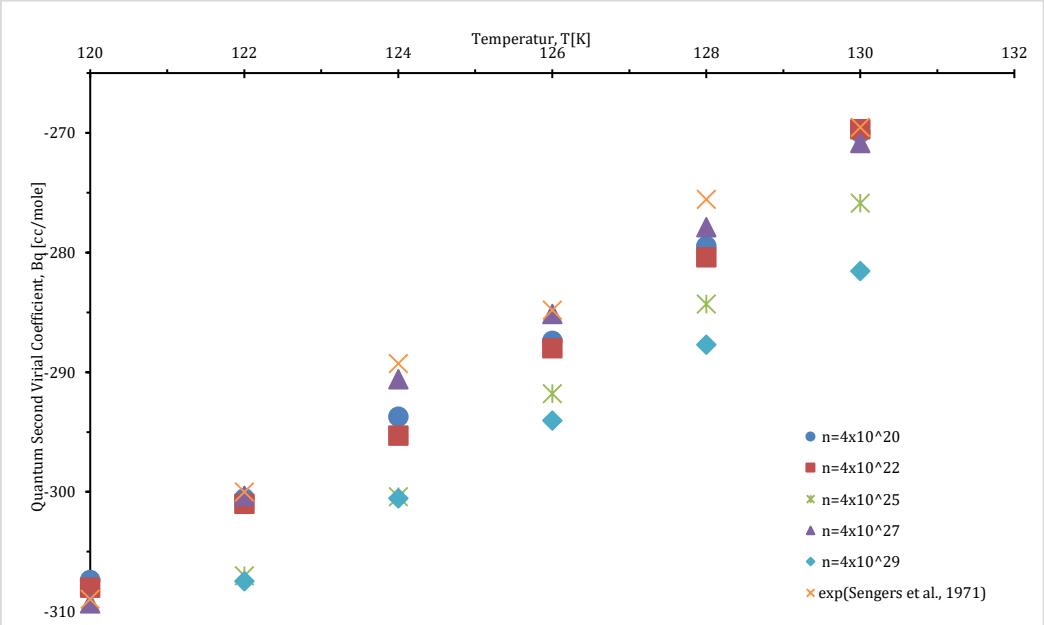

Fig. 1: Bq [cc/mole] as a function of temperature T [K] for different number densities n [atoms/m^3]

3.2. Pressure-volume-temperature (P-V-T) behavior

The 'virial equation of state' was usually written as (Feynman, 1998):

$$\frac{P}{nk_BT} = 1 + nB_q \quad (8)$$

The quantum second virial coefficient Bq can be fitted as a function of T. Its form is given as:

$$B_q = a + bT + cT^2 + dT^3 + eT^4 \quad (9)$$

where the fitting parameters calculated for $n = 4 \times 10^{25}$ atoms/m^3 are: $a = -437.82\ cm^3/mol$, $b = 4.18\ cm^3/(mol\ .K)$, $c = -0.02\ cm^3/(mol\ .K^2)$, $d = 5.123 \times 10^{-5} cm^3/(mol\ .K^3)$, e=-3.66×10^{-8}cm^3/(mol K^4).

Fig. 2 shows Bq and its fitting equation at $n = 4 \times 10^{25}$atoms/m^3. Clearly, the agreement is good in the present T-range.

In Fig. 3, the P-T curve indicates that P increases with increasing T, n being held fixed. Fig. 4 shows that P reaches a maximum and then decreases with increasing n. This is because the interatomic repulsive forces cause P to increase rapidly from a to b; whereas the attractive forces cause P to decrease equally rapidly from b to c (gas-liquid transition) (Kan, 1979).

Fig. 5 shows P as a function of V for two temperatures. One can see that if the system is compressed, V decreases until it reaches a critical volume V_c at a maximum pressure P_{max}. If the volume is decreased a little below V_c by compression to a pressure a little above P_{max}, this will lead to a collapse in the system and V and P decrease at the same time at a constant temperature. The system undergoes a gas-liquid phase transition at extremely low P and extremely low V (Koh, 2003). The critical physical quantities Vc and P_{max} are listed in Table 2 at two temperatures for n=0.4×10^{27}atoms/m^3.

3.3. Compressibility, Z

The Compressibility Factor Z, also known as the compression factor or the gas deviation factor, is a correction factor that describes the deviation of a real gas from ideal gas behavior. The compressibility factor is defined in thermodynamics as (Mosameh et al., 2014):

$$Z = 1 + nB_q(T) \quad (10)$$

Fig. 6 shows a plot of Z as a function of n for different temperatures: $120K$, $124K$ and$130\ K$. The

value of Z goes to 1 at very low density where $P \sim 0$, where all gases become ideal. As n increases, Z becomes less than 1 because of predominantly attractive forces. The gas becomes more and more ideal with increasing T, as expected.

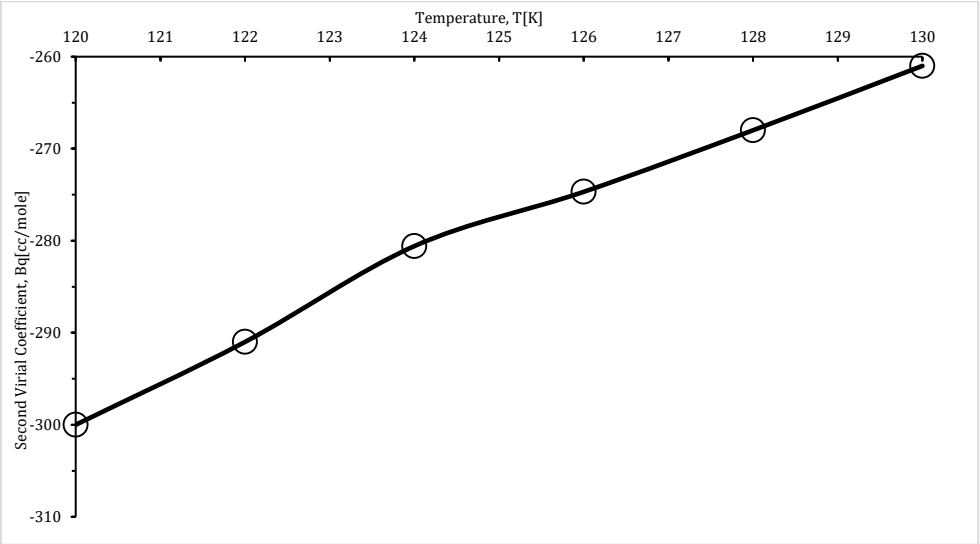

Fig. 2: The calculated Bq [cm³/mol] values and their fitting equation versus temperature T [K] at n= 4 ×10²⁵ atoms/m³

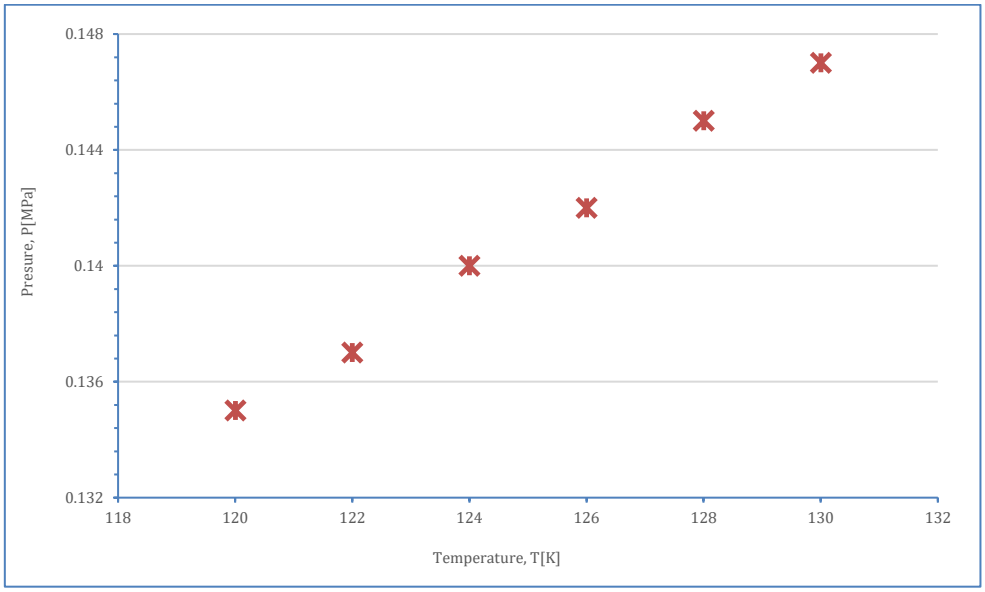

Fig. 3: The pressure P [MPa] as a function of temperature T [K] at n= 4 ×10²⁵ atoms/m³

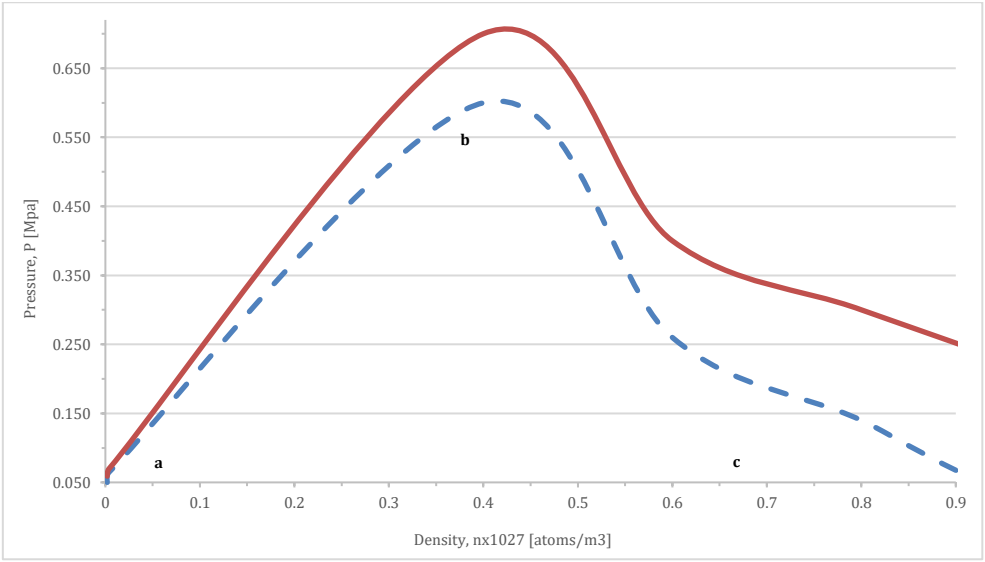

Fig. 4: The pressure P [MPa] as a function of number density n × 10²⁷ [atoms/m³] at t two temperatures T [K]

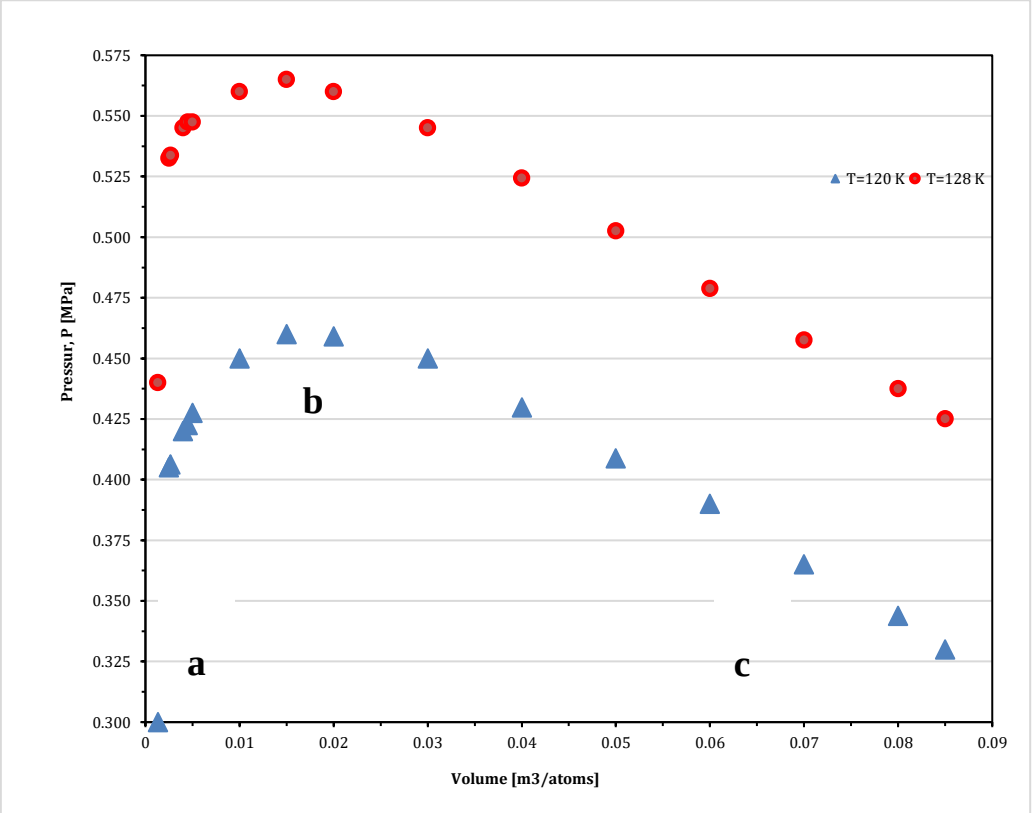

Fig. 5: The pressure P [MPa] as a function of volume V [m³/atoms] at two temperatures T [K]

Table 2: The critical volume V_c at the maximum pressure P_{max} [MPa] for two temperatures T [K], calculated from the virial equation of state for n=0.4×10²⁷atoms/m³

T [K]	Vc [m³/atoms]	P_{max} [MPa]
120	1.5 ×10⁻²	0.460
128	1.5 ×10⁻²	0.562

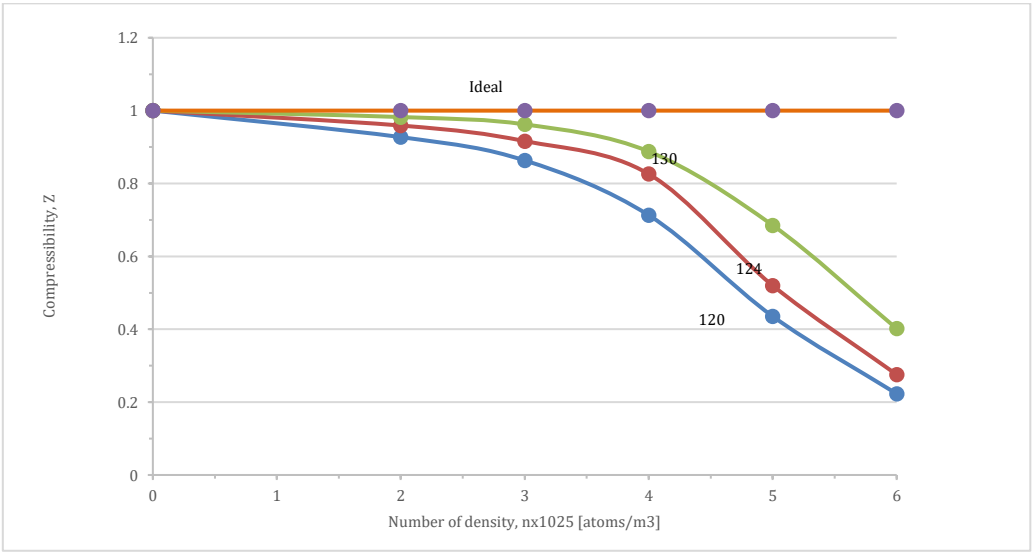

Fig. 6: The compressibility Z versus number density n [atoms/m³] at different temperatures T [K]

3.4. Other thermodynamic properties

After obtaining B, one can readily determine the internal energy U, the enthalpy H, and the Helmholtz free energy F as follows (Mozafari and Sharabadi, 2011; Mamedova and Somuncu, 2017):

$$U(T) \approx NK_B\left(\frac{3}{2}T - nT^2\frac{dB(T)}{dT}\right) \quad (11)$$

$$H = U + NK_BT(1 + nB(T)) \quad (12)$$

$$F = NK_BT[\ln\ (n\lambda^3) - 1 + nB(T)] \quad (13)$$

The results have been calculated for the number density n=4x10²⁵ atoms/m³. These results are displayed in Figs. 7-9. It was noted that U, H, and F increase with increasing T. This was because repulsive forces increase with increasing T.

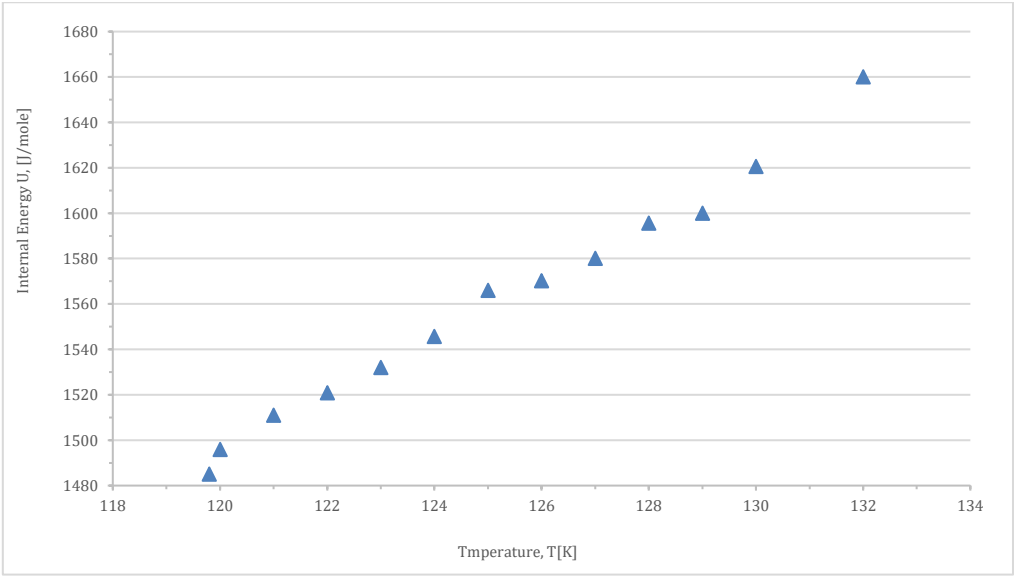

Fig. 7: The internal energy U [J/mol] as a function of temperature T [K] at n = $4x10^{25}$ atoms/m^3

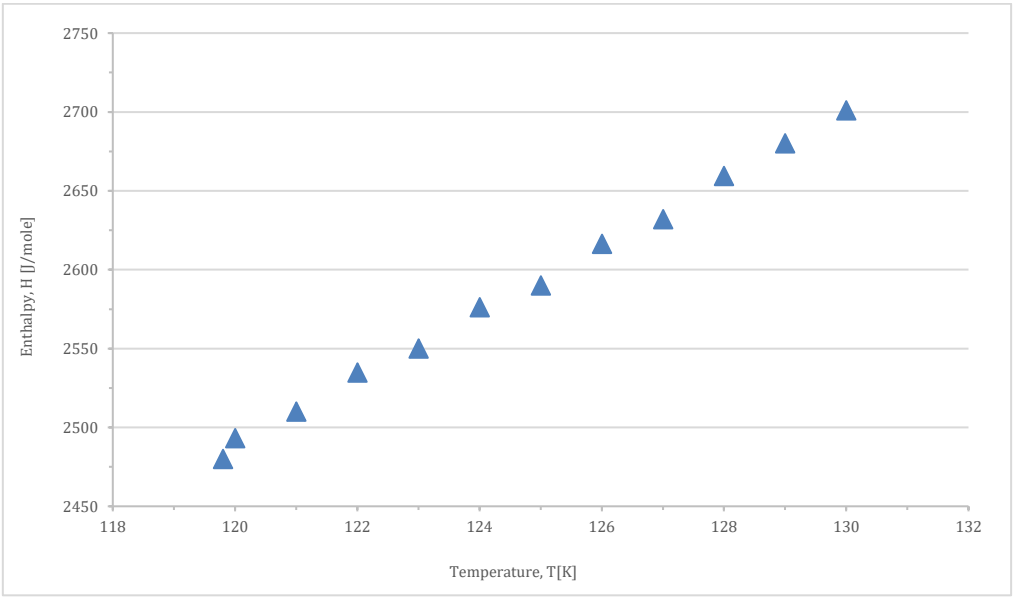

Fig. 8: The enthalpy H [J/mol] as a function of temperature T [K] at n = $4x10^{25}$ atoms/m^3

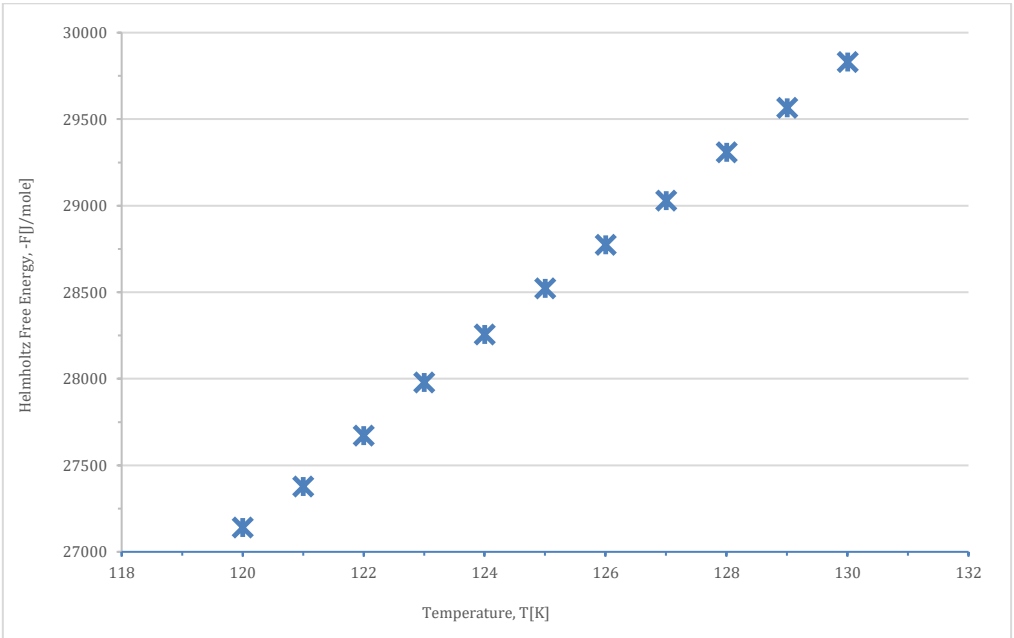

Fig. 9: The Helmholtz free energy F [J/mol] versus temperature T[K] at n = $4x10^{25}$ atoms/m^3

4. Conclusion

The many-body phase shifts for Kr gas are calculated for different number densities in the temperature-range 120-130 K, using the Galitskii-Migdal-Feynman formalism. These phase shifts are inserted in the Beth-Uhlenbeck formula to determine the quantum second virial coefficient Bq. Starting with B_q, standard expressions have been used to determine the thermodynamic properties of the system. It was noted that U, H, and F increase with increasing T. This was because repulsive forces increase with increasing T, and the gas becomes more and more ideal with decreasing n, as expected. The P–V–T behavior is carefully investigated, from which the phase (gas-liquid) transition is predicted. B_q is a good pointer to show the effect of the interatomic potential on the thermodynamic properties, particularly the pressure; i.e. when T decreases, the attractive forces between the interacting atoms increase, B_q becomes more negative, which leads the pressure to decrease and vice versa. On the other hand, B_q starts to decrease as the number density n increases.

Compliance with ethical standards

Conflict of interest

The author(s) declared no potential conflicts of interest with respect to the research, authorship, and/or publication of this article.

References

Akour AN, Sandouqa AS, Joudeh BR, and Ghassib HB (2018). Equation of state of ^{20}Ne gas in the temperature-range 27–36 K. Chinese Journal of Physics, 56(1): 411-422. https://doi.org/10.1016/j.cjph.2017.10.017

Al-Maaitah AF, Sandouqa AS, Joudeh BR, and Al-Obeidat OT (2019). The scattering and thermodynamic properties of ultracold ^{20}Ne vapor. Chinese Journal of Physics, 62: 194-201. https://doi.org/10.1016/j.cjph.2019.06.015

Al-Maaitah IF (2018). Quantum Second virial coefficients for Krypton-86 gas. Applied Physics Research, 10(1): 1-6. https://doi.org/10.12988/aap.2018.71210

Al-Maaitah IF, Joudeh BR, Sandouqa AS, and Ghassib HB (2016). Scattering properties of argon gas in the temperature range 87.3-120 K. Acta Physica Polonica A, 129(6): 1131-1140. https://doi.org/10.12693/APhysPolA.129.1131

Al-Obeidat OT (2021). Second virial coefficient of CH4 vapor in 5 mK-10000 K Temperature range in quantum and classical regimes. Acta Physica Polonica A, 139(2): 102-108. https://doi.org/10.12693/APhysPolA.139.102

Benseddik C, Bouazza MT, and Bouledroua M (2014). Thermophysical properties of a Krypton gas. Chinese Journal of Physics, 52(3): 1002-1014.

Bishop RF, Ghassib HB, and Strayer MR (1976). Composite pairs and effective two-body scattering in a many-body medium. Physical Review A, 13(4): 1570-1582. https://doi.org/10.1103/PhysRevA.13.1570

Byrne MA, Jones MR, and Staveley LAK (1968). Second virial coefficients of Argon, Krypton and Methane and their binary mixtures at low temperatures. Transactions of the Faraday Society, 64: 1747-1756. https://doi.org/10.1039/tf9686401747

Dardi PS and Dahler JS (1992). Classical and quantal calculations of the dimerization constant and second virial coefficient for argon. Theoretica Chimica Acta, 82(1): 117-129. https://doi.org/10.1007/BF01113133

Feynman RP (1998). Statistical mechanics: A set of lectures. 1st Edition, CRC Press, Boca Raton, USA.

Garberoglio G, Jankowski P, Szalewicz K, and Harvey AH (2012). Second virial coefficients of H2 and its isotopologues from a six-dimensional potential. The Journal of Chemical Physics, 137(15): 154308. https://doi.org/10.1063/1.4757565 **PMid:23083166**

Ghassib HB, Bishop RF, and Strayer MR (1976). A study of the Galitskii-Feynman *T* matrix for liquid ^{3}He. Journal of Low Temperature Physics, 23(3): 393-410. https://doi.org/10.1007/BF00116928

Ghassib HB, Sandouqa AS, Joudeh BR, and Mosameh SM (2014). Predicting the borderline between the classical and quantum regimes in ^{4}He gas from the second virial coefficient. Canadian Journal of Physics, 92(9): 997-1001. https://doi.org/10.1139/cjp-2013-0411

Joudeh BR, Sandouqa AS, Ghassib HB, and Al-Sugheir MK (2010). ^{3}He-^{3}He and ^{4}He-^{4}He cross sections in matter at low temperature. Journal of Low Temperature Physics, 161(3): 348-366. https://doi.org/10.1007/s10909-010-0211-6

Kan KC (1979). An equation of state and the gas-liquid-solid equilibrium in argon. Chinese Journal of Physics, 17(1): 32-43.

Koh SI (2003). Statistical mechanics of the gas–liquid condensation in the attractive Bose gas. Physica B: Condensed Matter, 329: 38-39. https://doi.org/10.1016/S0921-4526(02)01902-6

Mamedov BA and Somuncu E (2017). Accurate evaluation of the internal energy, free energy, entropy and enthalpy of non-polar molecules by using virial coefficients. Chinese Journal of Physics, 55(4): 1473-1488. https://doi.org/10.1016/j.cjph.2017.04.016

Mosameh SM, Sandouqa AS, Ghassib HB, and Joudeh BR (2014). Thermodynamic properties ^{4}He gas in the temperature range 4.2–10 K. Journal of Low Temperature Physics, 175(3): 523-542. https://doi.org/10.1007/s10909-013-1079-z

Mozafari F and Zare SZ (2011). Thermodynamic properties for Argon. Journal of Physical Chemistry and Electrochemistry, 1(3): 139-143.

Nezbeda I and Smith WR (2004). On the calculation of the critical temperature from the second virial coefficient. Fluid Phase Equilibria, 216(1): 183-186. https://doi.org/10.1016/j.fluid.2003.11.006

Oh SK (2010). Extending the group contribution concept using Kihara potential to perfluorinated n-alkanes C_nF_{2n+2} (n= 1–6) for estimating thermophysical properties. Fluid Phase Equilibria, 288(1-2): 87-95. https://doi.org/10.1016/j.fluid.2009.10.023

Sandouqa AS (2018). The quantum second virial coefficient as a predictor of formation of small spin-polarized tritium (T↓) clusters. Chemical Physics Letters, 703: 29-32. https://doi.org/10.1016/j.cplett.2018.05.010

Sandouqa AS, Joudeh BR, Al-Obeidat OT, Hawamdeh MM, and Ghassib HB (2020). A comprehensive study of the second virial coefficient of low-density ^{84}krypton vapor in the temperature range 0.01–700 K. The European Physical Journal Plus, 135(2): 1-12. https://doi.org/10.1140/epjp/s13360-020-00168-3

Seguin V, Guignes H, and Lhuillier C (1987). Virial calculations for H↓ in two and three dimensions. Physical Review B, 36: 141-155. https://doi.org/10.1103/PhysRevB.36.141 **PMid:9942034**

Sengers JMH, Klein M, and Gallagher JS (1971). Pressure-volume-temperature relationships of gases virial coefficients. Defense Technical Information Center, Fort Belvoir, USA.

Vliegenthart GA and Lekkerkerker HN (2000). Predicting the gas–liquid critical point from the second virial coefficient. The Journal of Chemical Physics, 112(12): 5364-5369. https://doi.org/10.1063/1.481106

Weir RD, Jones IW, Rowlinson JS, and Saville G (1967). Equation of state of gases at low temperatures; Part 1: Second virial coefficient of argon and krypton. Transactions of the Faraday Society, 63: 1320-1329. https://doi.org/10.1039/TF9676301320